



Cite this: *Chem. Commun.*, 2015, 51, 13408

Received 23rd June 2015,
Accepted 14th July 2015

DOI: 10.1039/c5cc05136c

www.rsc.org/chemcomm

Facile synthesis of multiple enzyme-containing metal–organic frameworks in a biomolecule-friendly environment†

Xiaoling Wu, Jun Ge,* Cheng Yang, Miao Hou and Zheng Liu

The one-step and facile synthesis of multi-enzyme-containing metal–organic framework (MOF) nanocrystals in aqueous solution at 25 °C was reported in this study. The GOx&HRP/ZIF-8 nanocomposite displayed high catalytic efficiency, high selectivity and enhanced stability due to the protecting effect of the framework.

Integration of enzymes, naturally evolved biocatalysts, as guest species into metal–organic frameworks¹ (MOFs) would give rise to artificial biocatalytic building blocks, promising for industrial biocatalysis, biosensing, and biomedical devices. Previous attempts to synthesize enzyme–MOF composites have been limited by the use of pre-synthesized special MOFs with large pores² or the use of organic solvent-resistant enzymes.³ Therefore, a facile and more general method for the synthesis of enzyme–MOF composites is urgently pursued to fully display the application spectrum of potentially numerous types of enzyme–MOF composites.

Recently, multi-enzyme systems involving a series of consecutive proceeding enzymatic reactions have attracted great attention,⁴ due to their important applications in the synthesis of pharmaceuticals,⁵ the fast diagnosis of diseases⁶ and the production of enzyme fuel cells.⁷ Promising strategies to construct artificial multi-enzyme systems include the utilization of DNA scaffolds,⁸ protein scaffolds,⁹ fusion proteins¹⁰ and various immobilization carriers.¹¹ Nanomaterials with large surface-to-volume ratios have been considered as promising carriers for multi-enzyme co-immobilization.¹²

In this study, we report the first example of a multiple enzyme-incorporated MOF, which can be readily prepared *via* a co-precipitation procedure in aqueous solution at ambient conditions. As shown in Fig. 1, the model cascade enzyme system of glucose oxidase (GOx) and horseradish peroxidase (HRP) was used to prepare the multiple enzyme-embedded

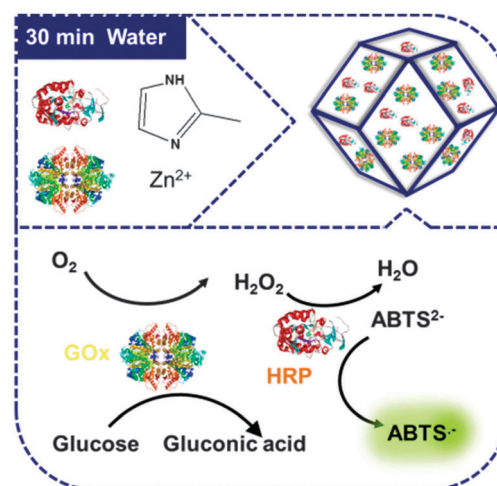


Fig. 1 Schematic synthesis of multi-enzyme-containing ZIF-8.

zeolitic imidazolate framework (ZIF-8). The GOx&HRP/ZIF-8 composite was formed within 30 min at 25 °C by simply mixing aqueous solutions containing zinc ions, 2-methylimidazole and enzymes. We hope that the use of water as the solvent would preserve the enzymes' activities well, and that the rigid structure of the MOF would increase the structural stability of the embedded enzymes, thus improving the enzymes' stabilities.

The synthesis of the multi-enzyme/ZIF-8 composite was performed by mixing zinc nitrate solution (0.31 M, 4 mL), enzyme solution (4 mL, 5 mg mL⁻¹ for GOx and 7.5 mg mL⁻¹ for HRP) and 2-methylimidazole (1.25 M, 40 mL) and stirring for 0.5 h at room temperature, followed by 3 cycles of centrifugation, at 6500 rpm for 5 min, and washing. As revealed in the scanning electron microscope (SEM) image (Fig. 2a), the product has an average size of around 500 nm and displays the same structure and morphology as the pure ZIF-8 crystals (Fig. 2b). The size of the nanocomposite was further confirmed by dynamic light scattering (DLS) (Fig. 2c), which agreed with the result of the SEM image and indicated a good dispersion of nanocomposites in methanol solution. Compared to the simulated XRD pattern¹³

Key Lab for Industrial Biocatalysis, Ministry of Education, Department of Chemical Engineering, Tsinghua University, Beijing 100084, China.

E-mail: junge@mails.tsinghua.edu.cn

† Electronic supplementary information (ESI) available: Synthesis of enzyme–MOF nanocrystals, SEM, TEM, CLSM characterizations and measurements of enzymatic performances. See DOI: 10.1039/c5cc05136c

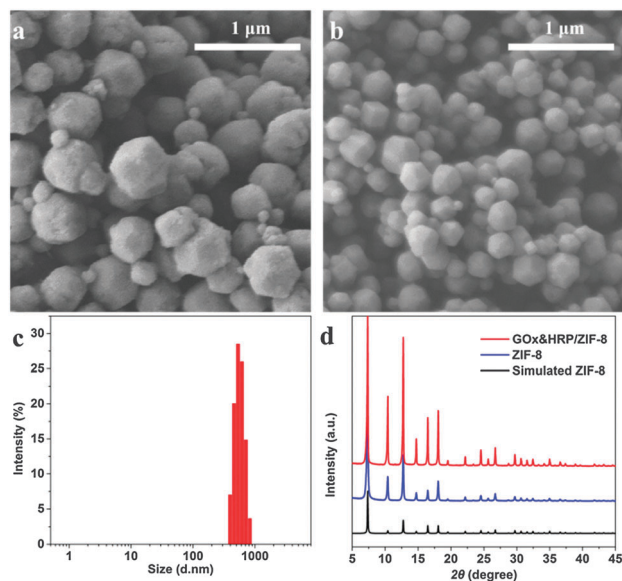


Fig. 2 SEM images of (a) the GOx&HRP/ZIF-8 composite, and (b) pure ZIF-8. (c) The particle size distribution of GOx&HRP/ZIF-8 determined by dynamic light scattering. (d) XRD patterns of simulated ZIF-8, pure ZIF-8 and GOx&HRP/ZIF-8 composite.

and the XRD pattern of the pure ZIF-8 (Fig. 2d), the similar XRD pattern of GOx&HRP/ZIF-8 indicated that the incorporation of enzyme did not affect the crystal structure of ZIF-8.

The transmission electron microscopy (TEM) image confirmed that the composite had a same morphology as the pure ZIF-8 (Fig. 3a and b). The energy dispersive X-ray spectroscopy (EDS) mapping (Fig. 3a) showed the existence and relatively uniform distribution of Fe element within the composite. As HRP is a ferric enzyme which contains one Fe ion in its heme group (Fe(III) in its ground state and catalysis reaction involves high-oxidation intermediates),¹⁴ the EDS results demonstrate that the

protein molecules were embedded in ZIF-8. To further confirm the incorporation of protein in ZIF-8, GOx and HRP were labeled with fluorescent probes fluorescein isothiocyanate (FITC) and rhodamine B isothiocyanate (RhB), respectively, and subjected to the same procedure to synthesize the protein/ZIF-8 composite. From the confocal laser scanning microscopy (CLSM) (Fig. 3c, right column, single channel mode of CLSM), it can be observed that both FITC-GOx (green) and RhB-HRP (red) were present in ZIF-8. It seems that FITC-GOx tends to localize on the outer region of the ZIF-8 crystals while RhB-HRP tends to localize inside (Fig. 3c, left column, multiple channel mode). The thermal gravity analysis (TGA) in air also confirmed the presence of protein in the composite (Fig. 3d). The first-stage decomposition of both the composite and pure ZIF-8 in air exhibited a gradual weight loss of ~15% up to ca. 200 °C corresponding to the removal of guest molecules (mostly H₂O and other organic small molecules) from the cavities and some unreacted reagents. The second decomposition stage of the composite started from 250 °C and finished around 350 °C, while the pure ZIF-8 crystals had much less weight loss during this temperature range.¹⁵ About 10 wt% of weight loss of the composite occurred during the second stage, which can be attributed to the decomposition of protein molecules. Size exclusion chromatography (SEC) was applied to determine the amounts of the residual GOx and HRP molecules in the supernatant after synthesis of the composite (Fig. S1, ESI[†]), from which the loading amount of GOx and HRP in the composite was calculated as 4 wt% and 6 wt% respectively. This agreed well with the 10 wt% of weight loss in the TGA analysis.

The catalytic efficiency of the GOx&HRP/ZIF-8 composite was evaluated by the detection of glucose using 2,2'-azino-bis(3-ethylbenzothiazoline-6-sulphonic acid) (ABTS) as a chromogenic substrate. As shown in Fig. 1, GOx converts glucose into gluconic acid and generates H₂O₂ which is the substrate for HRP to oxidize ABTS²⁻ to form ABTS^{•+} which is detectable at 415 nm. In a typical experiment, the absorbance at 415 nm was measured after 10 min incubation of 0.75 mg mL⁻¹ of GOx&HRP/ZIF-8 composite in phosphate buffer saline (PBS) containing glucose (0–100 μM) and ABTS (532 μM) at room temperature. As shown in Fig. 4a, a good linearity between the absorbance and the concentration of glucose in the range of 0–100 μM was obtained ($R^2 = 0.991$). The limit of detection (LOD) is 0.5 μM, lower than most of the reported colorimetric glucose sensors.¹⁶ In addition, a direct visible detection can be achieved by using GOx&HRP/ZIF-8 composite in solution (Fig. 4a, inset). Moreover, by depositing the GOx&HRP/ZIF-8 composite on round pieces of filter paper (6 mm in diameter), this multi-enzyme-containing testing strip can be used for the convenient detection of glucose in a droplet of 20 μL (Fig. 4a, inset). The advantages of facile detection, high sensitivity, and operation with an ultra-small amount of sample could be promising for developing the next-generation glucose biosensors for possible non-invasive detection of glucose in tears, urine, and sweat.¹⁷ Moreover, the ZIF-8 itself showed no activity towards glucose (Fig. S3, ESI[†]). The performance of the GOx&HRP/ZIF-8 was compared to that of a mixture of GOx/ZIF-8 and HRP/ZIF-8 with the same protein content. The GOx&HRP/ZIF-8 composite showed 2 times higher activity than the mixture

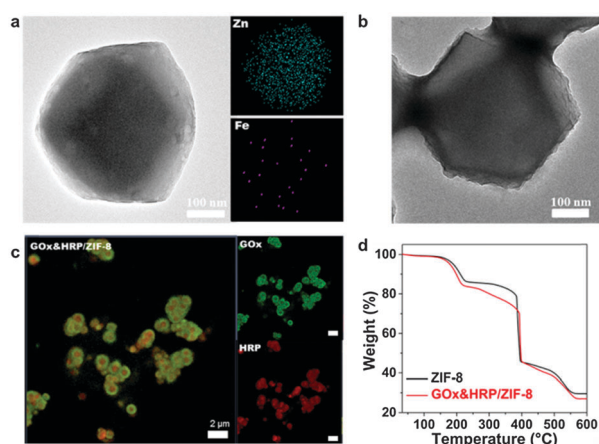


Fig. 3 (a) TEM image of GOx&HRP/ZIF-8 composite and EDS mapping of elemental distributions for Zn and Fe. (b) TEM image of pure ZIF-8. (c) Confocal microscopy image of the GOx&HRP/ZIF-8 composite (left column), HRP was labeled with RhB (red) (right column) and GOx was labeled with FITC (green) (right column), the scale bar is 2 μm. (d) TGA curves of the GOx&HRP/ZIF-8 composite and ZIF-8 in air.

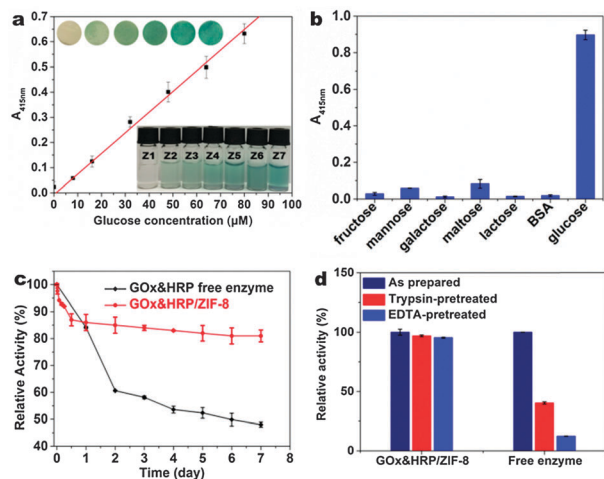


Fig. 4 (a) Detection of glucose in solution at concentrations of 0–100 μM (absorbance at 415 nm was measured after incubation in solution for 10 min at room temperature), inset: photographs showing visible detection of glucose by enzyme-containing paper strips and in solution (for the paper strip testing, 20 μL of aqueous solution containing 100 μM , 500 μM , 1 mM, 2 mM, 5 mM, 8 mM of glucose was applied on the surface of paper strip followed by reaction for 15 min at room temperature; for the visible detection in pH 7.4 phosphate buffer saline solution, the concentration of glucose for Z1–Z7 was 0, 8, 16, 32, 48, 64, 80 μM , respectively). (b) Determination of the selectivity of the GOx&HRP/ZIF-8 composite (the solution contains 1.0 mM of fructose, 1.0 mM of mannose, 1.0 mM of galactose, 1.0 mM of maltose, 1.0 mM of lactose, 1 mg mL^{-1} of BSA and 100 μM of glucose, respectively). (c) Long-term stability of the GOx&HRP/ZIF-8 composite compared with free enzymes incubated in pH 7.4 phosphate buffer saline solution at room temperature. (d) Stability of the GOx&HRP/ZIF-8 composite compared with free enzymes incubated in pH 7.4 phosphate buffer saline solution containing 1 mg mL^{-1} of trypsin or 1 wt% of EDTA.

of the GOx/ZIF-8 and HRP/ZIF-8 composites, at the same glucose concentration (Fig. S3, ESI[†]). This activity enhancement might be ascribed to the more complete and immediate utilization of the intermediate (H_2O_2) produced in the multi-enzyme–MOF system due to the proximity of the enzymes. In the case of the mixture of the GOx/ZIF-8 and HRP/ZIF-8 composite, the intermediate needs to transfer out from the GOx/ZIF-8 framework and then enter HRP/ZIF-8.

The selectivity of the GOx&HRP/ZIF-8 composite for glucose was evaluated by monitoring the absorbance at 415 nm in the presence of various interfering compounds including fructose, mannose, galactose, maltose, lactose and albumin. As shown in Fig. 4b, even at concentrations of these compounds that were 10-times higher compared to the concentration of glucose, the GOx&HRP/ZIF-8 composite didn't show an obvious activity towards these interfering compounds, demonstrating its high selectivity towards glucose.

The long-term storage stability of enzymes is another important aspect for developing a reliable biosensor. As shown in Fig. 4c, after completely washing out the enzyme bound on the surface of MOF crystals by DI water 6 times, the GOx&HRP/ZIF-8 showed a gradual decrease of overall activity ($\sim 15\%$) during the first day when incubated in PBS at room temperature, which might be due to the inherent instability of protein. After that, the GOx&HRP/ZIF-8 retained $\sim 80\%$ of initial overall activity

for 7 days. In contrast, the free enzyme system (GOx&HRP) in solution at the same condition lost nearly 50% of the overall activity within 2 days. ZIF-8 can maintain its full crystallinity even after boiling in water for 7 days.¹³ The high chemical and structural stability of ZIF-8 provides the protecting effect for the encapsulated enzymes during long-term storage. The confinement of the proteins within the rigid crystal structure of ZIF-8 prevents protein denaturation caused by thermal fluctuations of proteins in solution. The multi-enzyme/ZIF-8 composite can be reused by centrifugation. The relative activity of the multi-enzyme/ZIF-8 decreased to less than 20% after 4 cycles (Fig. S4, ESI[†]). The obvious loss of activity can be ascribed to the nanometer size of the composite and its good dispersability in aqueous solution, which resulted in partial recovery of the composite by centrifugation. The controlled synthesis of larger composites in micrometer size might be worthy of investigation to address this problem.

The stability of enzymes *in vivo* is essentially important for developing the implanted glucose biosensors.¹⁸ Degradation by digestive enzymes and deactivation of GOx and HRP in the presence of chelating compounds are two major reasons among others accounting for the poor stability of enzymes *in vivo*. Here the stability of the GOx&HRP/ZIF-8 composite against protease and ethylenediaminetetraacetic acid (EDTA) as the model digesting enzyme and chelating compound, respectively, was examined. As shown in Fig. 4d, free GOx and HRP lost nearly half of their overall activity after being digested by trypsin for 30 min at 37 $^\circ\text{C}$. The GOx&HRP/ZIF-8 composite retained almost the same activity in the same condition, demonstrating an excellent tolerance against digesting enzymes. Similarly, the GOx&HRP/ZIF-8 composite in the presence of 1 wt% of EDTA retained 95% of its original activity whereas the free enzyme system lost 90% of its original activity, exemplifying a shielding function of the MOF scaffold against chelating compounds.

In summary, we presented a one-step, facile and general method for the aqueous synthesis of multiple enzyme-containing ZIF-8 nanocrystals using GOx and HRP as model enzymes. The structural rigidity and confinement of the MOF scaffolds greatly enhanced the thermal stability of the embedded enzymes and moreover, shielded the embedded enzymes from proteolysis and chelating. It was demonstrated that the composite has a high overall catalytic efficiency for an enzyme cascade reaction. The high sensitivity, selectivity, long-term storage stability and stability of the GOx&HRP/ZIF-8 nanocomposite against digesting enzymes and chelating compounds make it promising for developing reliable glucose biosensors. The ease of operation of this method is appealing for the fabrication of various types of MOF-based building blocks containing multiple biological components for applications in biotechnology, industrial biocatalysis, biosensing and biomedical engineering.

This work was supported by the National High Technology Research and Development Program ("863" Program) of China under the grant number of 2014AA020507, the National Natural Science Foundation of China under the grant numbers 21206082, the Beijing Natural Science Foundation under the grant number of 2144050 and the Tsinghua University Initiative Scientific Research Program under the grant number of 20131089191.

Notes and references

- (a) H. Furukawa, K. E. Cordova, M. O'Keeffe and O. M. Yaghi, *Science*, 2013, **341**, 1230444; (b) O. K. Farha and J. T. Hupp, *Acc. Chem. Res.*, 2010, **43**, 1166; (c) J.-P. Zhang, Y.-B. Zhang, J.-B. Lin and X.-M. Chen, *Chem. Rev.*, 2011, **112**, 1001; (d) G. Li, H. Kobayashi, J. M. Taylor, R. Ikeda, Y. Kubota, K. Kato, M. Takata, T. Yamamoto, S. Toh and S. Matsumura, *Nat. Mater.*, 2014, **13**, 802; (e) P. K. Thallapally, J. Tian, M. Radha Kishan, C. A. Fernandez, S. J. Dalgarno, P. B. McGrail, J. E. Warren and J. L. Atwood, *J. Am. Chem. Soc.*, 2008, **130**, 16842; (f) F. Zhang, Y. Wei, X. Wu, H. Jiang, W. Wang and H. Li, *J. Am. Chem. Soc.*, 2014, **136**, 13963; (g) Z. Zhang, Y. Chen, S. He, J. Zhang, X. Xu, Y. Yang, F. Nosheen, F. Saleem, W. He and X. Wang, *Angew. Chem.*, 2014, **126**, 12725; (h) Z.-Z. Lu, R. Zhang, Y.-Z. Li, Z.-J. Guo and H.-G. Zheng, *J. Am. Chem. Soc.*, 2011, **133**, 4172.
- (a) Y. Chen, V. Lykourinou, C. Vetromile, T. Hoang, L.-J. Ming, R. W. Larsen and S. Ma, *J. Am. Chem. Soc.*, 2012, **134**, 13188; (b) V. Lykourinou, Y. Chen, X.-S. Wang, L. Meng, T. Hoang, L.-J. Ming, R. L. Musselman and S. Ma, *J. Am. Chem. Soc.*, 2011, **133**, 10382; (c) D. Feng, T.-F. Liu, J. Su, M. Bosch, Z. Wei, W. Wan, D. Yuan, Y.-P. Chen, X. Wang, K. Wang, X. Lian, Z.-Y. Gu, J. Park, X. Zou and H.-C. Zhou, *Nat. Commun.*, 2015, **6**, 5979.
- F. Lyu, Y. Zhang, R. N. Zare, J. Ge and Z. Liu, *Nano Lett.*, 2014, **14**, 5761.
- (a) P. Kallio, A. Pásztor, K. Thiel, M. K. Akhtar and P. R. Jones, *Nat. Commun.*, 2014, **5**, 4731; (b) B. T. Ueberbacher, M. Hall and K. Faber, *Nat. Prod. Rep.*, 2012, **29**, 337; (c) J. C. Carlson, S. Li, S. S. Gunatilleke, Y. Anzai, D. A. Burr, L. M. Podust and D. H. Sherman, *Nat. Chem.*, 2011, **3**, 628.
- (a) E. O'Reilly, C. Iglesias, D. Ghislieri, J. Hopwood, J. L. Galman, R. C. Lloyd and N. J. Turner, *Angew. Chem., Int. Ed.*, 2014, **53**, 2447; (b) R. J. Fox, S. C. Davis, E. C. Mundorff, L. M. Newman, V. Gavrilovic, S. K. Ma, L. M. Chung, C. Ching, S. Tam, S. Muley, J. Grate, J. Gruber, J. C. Whitman, R. A. Sheldon and G. W. Huisman, *Nat. Biotechnol.*, 2007, **25**, 338; (c) S. K. Ma, J. Gruber, C. Davis, L. Newman, D. Gray, A. Wang, J. Grate, G. W. Huisman and R. A. Sheldon, *Green Chem.*, 2010, **12**, 81.
- J. Galban, V. Sanz and S. de Marcos, *Biosens. Bioelectron.*, 2007, **22**, 2876.
- (a) Z. Zhu, T. Kin Tam, F. Sun, C. You and Y. H. Percival Zhang, *Nat. Commun.*, 2014, **5**, 3026; (b) Z.-G. Wang, O. I. Wilner and I. Willner, *Nano Lett.*, 2009, **9**, 4098.
- (a) O. I. Wilner, Y. Weizmann, R. Gill, O. Lioubashevski, R. Freeman and I. Willner, *Nat. Nanotechnol.*, 2009, **4**, 249; (b) J. Fu, Y. R. Yang, A. Johnson-Buck, M. Liu, Y. Liu, N. G. Walter, N. W. Woodbury and H. Yan, *Nat. Nanotechnol.*, 2014, **9**, 531; (c) Y. Liu, J. Du, M. Yan, M. Y. Lau, J. Hu, H. Han, O. O. Yang, S. Liang, W. Wei, H. Wang, J. Li, X. Zhu, L. Shi, W. Chen, C. Ji and Y. Lu, *Nat. Nanotechnol.*, 2013, **8**, 187.
- J. E. Dueber, G. C. Wu, G. R. Malmirchegini, T. S. Moon, C. J. Petzold, A. V. Ullal, K. L. J. Prather and J. D. Keasling, *Nat. Biotechnol.*, 2009, **27**, 753.
- (a) H. Hirakawa and T. Nagamune, *ChemBioChem*, 2010, **11**, 1517; (b) X. Gao, S. Yang, C. Zhao, Y. Ren and D. Wei, *Angew. Chem.*, 2014, **126**, 14251.
- (a) H. Bäumler and R. Georgieva, *Biomacromolecules*, 2010, **11**, 1480; (b) A. Grotzky, T. Nausser, H. Erdogan, A. D. Schlüter and P. Walde, *J. Am. Chem. Soc.*, 2012, **134**, 11392; (c) M. Zheng, Z. Su, X. Ji, G. Ma, P. Wang and S. Zhang, *J. Biotechnol.*, 2013, **168**, 212; (d) J. Shi, X. Wang, Z. Jiang, Y. Liang, Y. Zhu and C. Zhang, *Bioresour. Technol.*, 2012, **118**, 359; (e) Q. Dong, L.-M. Ouyang, H.-L. Yu and J.-H. Xu, *Carbohydr. Res.*, 2010, **345**, 1622.
- (a) R. A. Sheldon and S. van Pelt, *Chem. Soc. Rev.*, 2013, **42**, 6223; (b) M. Hartmann and X. Kostrov, *Chem. Soc. Rev.*, 2013, **42**, 6277; (c) Y. Lin, J. Ren and X. Qu, *Acc. Chem. Res.*, 2014, **47**, 1097; (d) Y. Lin, C. Xu, J. Ren and X. Qu, *Angew. Chem., Int. Ed.*, 2012, **51**, 12579.
- K. S. Park, Z. Ni, A. P. Côté, J. Y. Choi, R. Huang, F. J. Uribe-Romo, H. K. Chae, M. O'Keeffe and O. M. Yaghi, *Proc. Natl. Acad. Sci. U. S. A.*, 2006, **103**, 10186.
- G. I. Berglund, G. H. Carlsson, A. T. Smith, H. Szöke, A. Henriksen and J. Hajdu, *Nature*, 2002, **417**, 463.
- Y. Pan, Y. Liu, G. Zeng, L. Zhao and Z. Lai, *Chem. Commun.*, 2011, **47**, 2071.
- (a) J. Mu, Y. Wang, M. Zhao and L. Zhang, *Chem. Commun.*, 2012, **48**, 2540; (b) Y. Song, K. Qu, C. Zhao, J. Ren and X. Qu, *Adv. Mater.*, 2010, **22**, 2206; (c) H. Wei and E. Wang, *Anal. Chem.*, 2008, **80**, 2250; (d) Q. Yan, B. Peng, G. Su, B. E. Cohan, T. C. Major and M. E. Meyerhoff, *Anal. Chem.*, 2011, **83**, 8341.
- (a) V. L. Alexeev, S. Das, D. N. Finegold and S. A. Asher, *Clin. Chem.*, 2004, **50**, 2353; (b) J. Kost, S. Mitragotri, R. A. Gabbay, M. Pishko and R. Langer, *Nat. Med.*, 2000, **6**, 347.
- (a) L. Fang, B. Liang, G. Yang, Y. Hu, Q. Zhu and X. Ye, *Biosens. Bioelectron.*, 2014, **56**, 91; (b) M. C. Frost and M. E. Meyerhoff, *Curr. Opin. Chem. Biol.*, 2002, **6**, 633.